Published OnlineFirst April 13, 2010; DOI:10.1158/1078-0432.CCR-09-2214

leading to the formation of two microtubule asters that do not form a spindle (27). TPX2 is necessary for maintaining aurora A kinase in an active conformation (28, 29). Aurora kinases are essential for the regulation of chromosome segregation and cytokinesis during mitosis and have been reported to be overexpressed in a wide range of human tumors. Several aurora kinase inhibitors, such as VX-680/MK-0457, have been showed to have anticancer effects *in vitro* and *in vivo* (30, 31). The binding of TPX2 modulates the conformation of aurora A and reduces its affinity

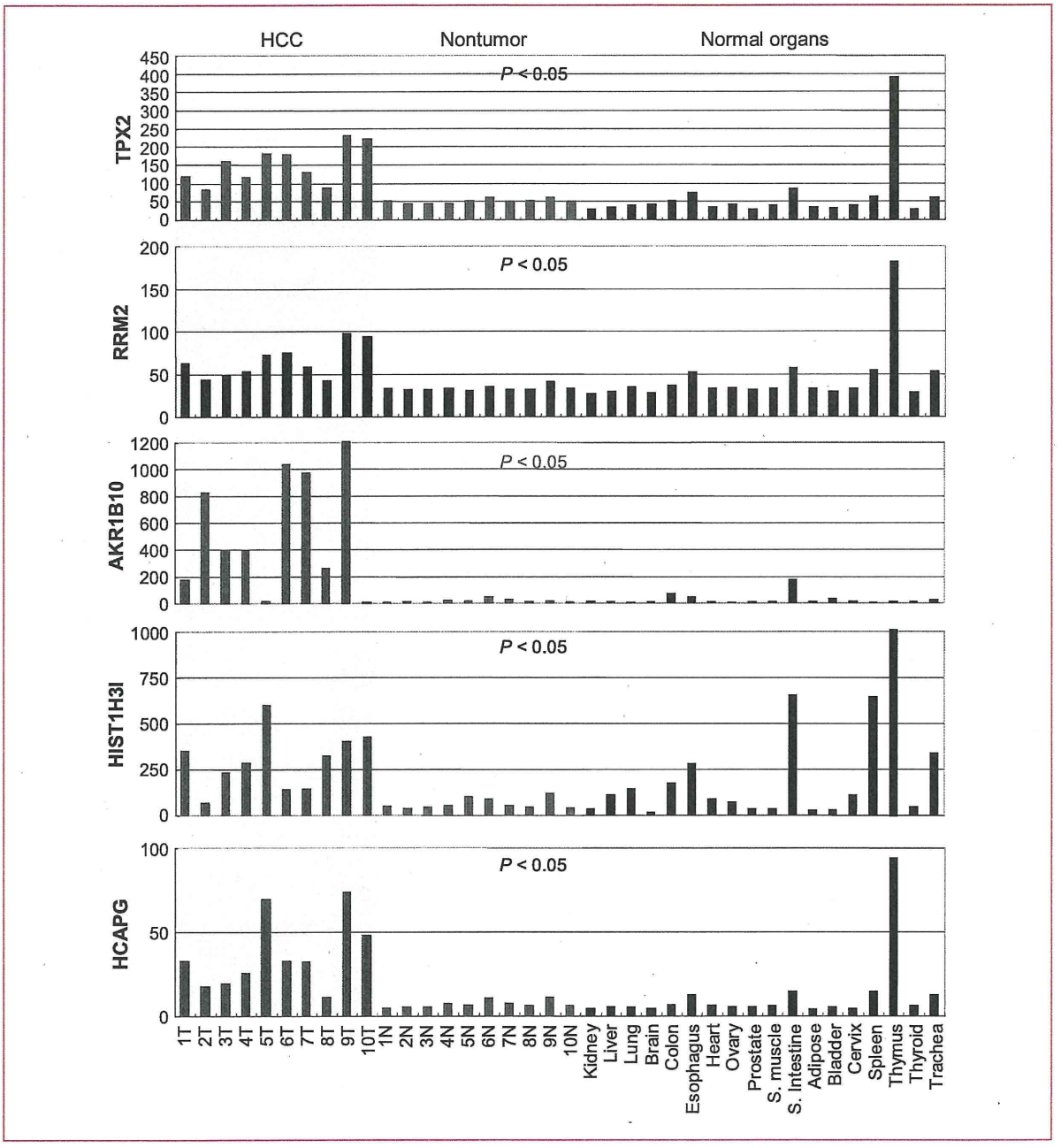

Fig. 4. Expression in normal organs. Expression levels of mRNAs for selected genes in 10 pairs of HCC (1-10T) and adjacent nontumorous liver tissue (1-10N; discovery set 1) and 18 normal organs determined by Human Exon 1.0 ST arrays (shown in arbitrary units). The significance of differential expression between HCC and adjacent nontumorous liver tissue was assessed using permutation paired *t* test, and Bonferroni-corrected *P* values are provided. S. muscle, skeletal muscle; S. intestine, small intestine.

Published OnlineFirst April 13, 2010; DOI:10.1158/1078-0432.CCR-09-2214

for VX-680 (32). Inhibition of TPX2 may increase the efficacy of this class of aurora kinase inhibitors.

HCAP-G is a component of the condensin complex that organizes the coiling topology of individual chromatids. Condensin also contributes to mitosis-specific chromosome compaction and is required for proper chromosome segregation, although the functional significance of HCAP-G in the condensing complex is largely unknown (33, 34).

AKR1B10 (ARL1, aldose reductase-like 1) was originally isolated as a new member of the aldo-keto reductase superfamily overexpressed in HCC and is reportedly related to the histologic differentiation of HCC (35, 36). AKR1B10 was also overexpressed in squamous cell carcinoma of the lung and its precursor conditions (37). Because the expression of AKR1B10 was highly specific to HCC and its inhibition suppressed tumor growth (Fig. 6), chemicals that specifically inhibit AKR1B10 activity may be useful anticancer drugs with minimal side effects.

It cannot be denied that many important genes were probably overlooked at every step of the present screen,

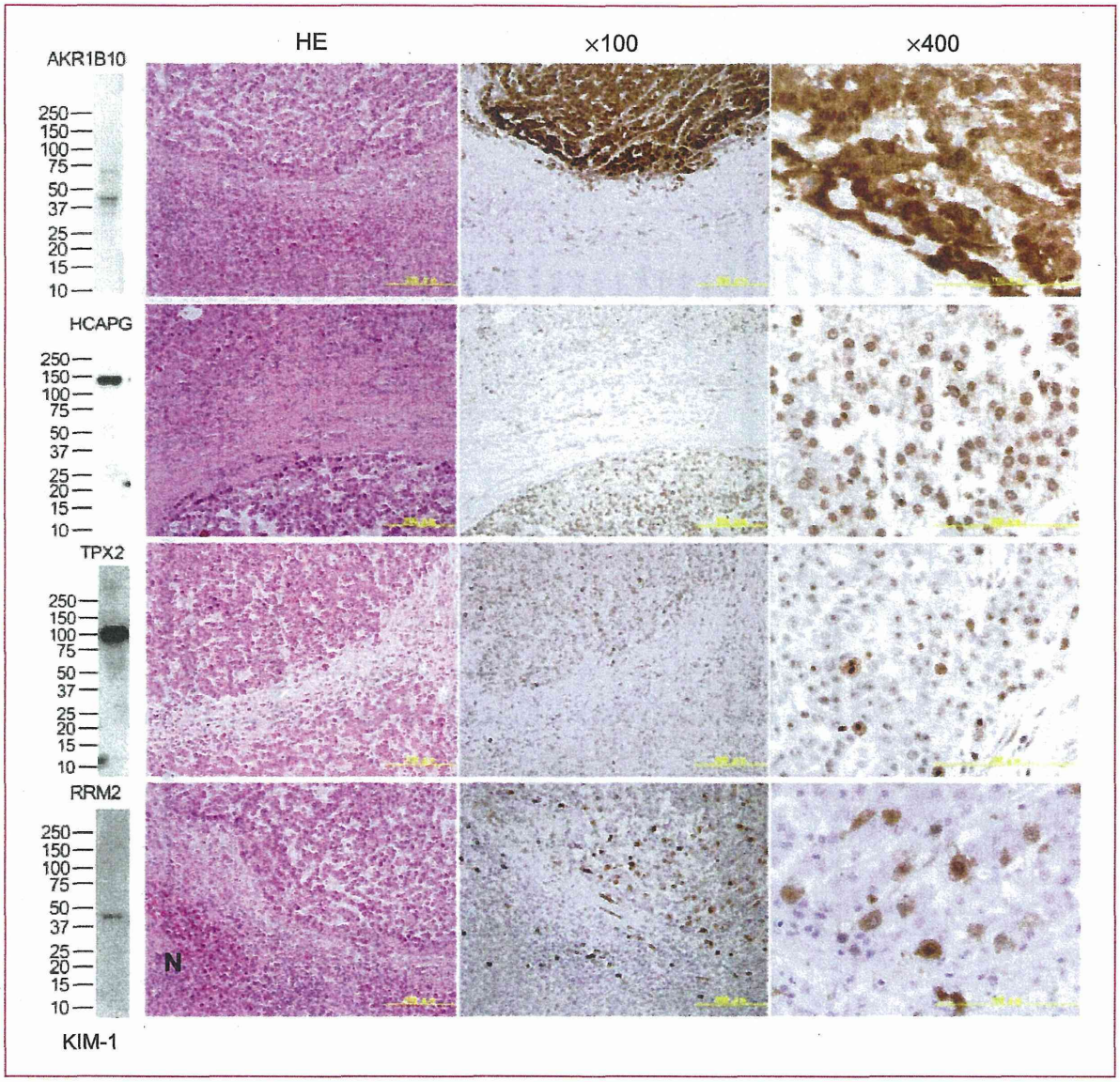

Fig. 5. Protein expression in HCC. Hematoxylin and eosin (HE) staining (original magnification, × 100) and immunoperoxidase staining (original magnifications, × 100 and × 400) of AKR1B10, HCAP-G, RRM2, and TPX2 proteins in HCC and adjacent nontumorous liver tissue. The specificity of antibodies was determined by immunoblotting of the KIM-1 cell lysate (left). N, nontumorous liver.

Published OnlineFirst April 13, 2010; DOI:10.1158/1078-0432.CCR-09-2214

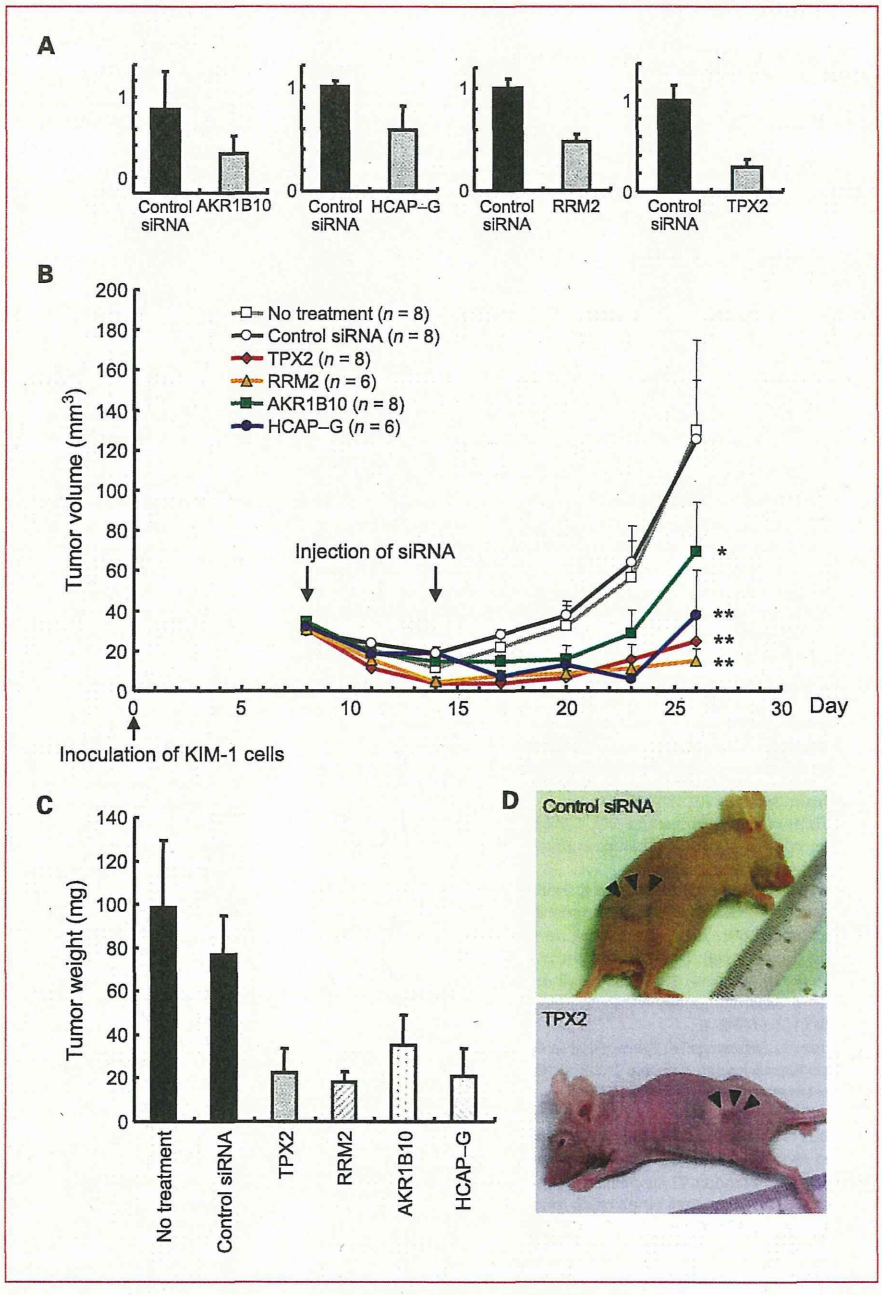

Fig. 6. Suppression of tumor growth by siRNA. A, KIM-1 cells were s.c. inoculated into the flanks of nude mice. Eight days later, control siRNA or siRNA against *AKR1B10, HCAP-G, RRM2*, or *TPX2* was injected into the developed tumors. The tumors were excised 2 days after the injection, and the expression levels of the indicated genes were determined by real-time PCR. Values of control siRNA were set at 1. B, chronological changes in tumor volume after two injections of the indicated siRNA. Volume of tumors was determined every 3 days as described in Materials and Methods. **, significantly different with a Bonferroni-corrected *P* value of <0.001. *, significantly different with a Bonferroni-corrected *P* value of 0.012. C, weight (mean + SE in mg) of xenografts measured 18 days after the second injection of the indicated siRNA and controls. D, macroscopic appearance of xenografts injected with control siRNA (top) and siRNA against TPX2 (bottom).

although the four selected genes seem to be highly relevant from a biological viewpoint. HCC has been recognized as a single category of disease; however, the overall gene expression patterns seem to differ markedly among individual cases. A search for the genes responsible for the different clinical outcomes of HCC will be the subject of a future study. We used the cell proliferation assay for siRNA-based functional screening. However, the use of other assays capable of evaluating cell motility, migration, drug sensitivity, or cell death may help to identify genes differing in their biological significance. The combination of genome-wide expression and functional screening described here provides a rapid and comprehensive approach that could be applicable for studies of various aspects of human cancer.

Disclosure of Potential Conflicts of Interest

No potential conflicts of interest were disclosed.

Published OnlineFirst April 13, 2010; DOI:10.1158/1078-0432.CCR-09-2214

Acknowledgments

We thank Dr. Masamichi Kojiro (Kurume University, Kurume, Japan) for providing the KIM-1 cells.

Grant Support

Program for Promotion of Fundamental Studies in Health Sciences conducted by the National Institute of Biomedical Innovation of Japan, the Third-Term Comprehensive Control Research for Cancer conducted by the Ministry of Health, Labor and Welfare of Japan, and generous grants from the Natio Foundation and the Princess Takamatsu Cancer Research Fund. These fund resources did not influence the study design or interpretation of the results.

The costs of publication of this article were defrayed in part by the payment of page charges. This article must therefore be hereby marked *advertisement* in accordance with 18 U.S.C. Section 1734 solely to indicate this fact.

Received 08/15/2009; revised 02/01/2010; accepted 03/08/2010; published OnlineFirst 04/13/2010.

References

1. El-Serag HB, Rudolph KL. Hepatocellular carcinoma: epidemiology and molecular carcinogenesis. Gastroenterology 2007;132:2557–76.
2. Hernandez-Boluda JC, Cervantes F. Imatinib mesylate (Gleevec, Glivec):a new therapy for chronic myeloid leukemia and other malignancies. Drugs Today (Barc) 2002;38:601–13.
3. Fong T, Morgensztern D, Govindan R. EGFR inhibitors as first-line therapy in advanced non-small cell lung cancer. J Thorac Oncol 2008;3:303–10.
4. Llovet JM, Ricci S, Mazzaferro V, et al. Sorafenib in advanced hepatocellular carcinoma. N Engl J Med 2008;359:378–90.
5. Di Maio M, Daniele B, Perrone F. Targeted therapies: role of sorafenib in HCC patients with compromised liver function. Nat Rev Clin Oncol 2009;6:505–6.
6. Hideshima T, Chauhan D, Richardson P, Anderson KC. Identification and validation of novel therapeutic targets for multiple myeloma. J Clin Oncol 2005;23:6345–50.
7. Izzo F, Marra P, Beneduce G, et al. Pegylated arginine deiminase treatment of patients with unresectable hepatocellular carcinoma: results from phase I/II studies. J Clin Oncol 2004;22:1815–22.
8. Drew Y, Plummer R. The emerging potential of poly(ADP-ribose) polymerase inhibitors in the treatment of breast cancer. Curr Opin Obstet Gynecol 2010;22:67–71.
9. Whitehurst AW, Bodemann BO, Cardenas J, et al. Synthetic lethal screen identification of chemosensitizer loci in cancer cells. Nature 2007;446:815–9.
10. Silva JM, Marran K, Parker JS, et al. Profiling essential genes in human mammary cells by multiplex RNAi screening. Science 2008;319:617–20.
11. Schlabach MR, Luo J, Solimini NL, et al. Cancer proliferation gene discovery through functional genomics. Science 2008;319:620–4.
12. Luo B, Cheung HW, Subramanian A, et al. Highly parallel identification of essential genes in cancer cells. Proc Natl Acad Sci U S A 2008;105:20380–5.
13. Huang L, Shitashige M, Satow R, et al. Functional interaction of DNA topoisomerase IIα with the β-catenin and T-cell factor-4 complex. Gastroenterology 2007;133:1569–78.
14. Shitashige M, Naishiro Y, Idogawa M, et al. Involvement of splicing factor-1 in β-catenin/T-cell factor-4-mediated gene transactivation and pre-mRNA splicing. Gastroenterology 2007;132:1039–54.
15. Honda K, Yamada T, Hayashida Y, et al. Actinin-4 increases cell motility and promotes lymph node metastasis of colorectal cancer. Gastroenterology 2005;128:51–62.
16. Yamaguchi U, Nakayama R, Honda K, et al. Distinct gene expression-defined classes of gastrointestinal stromal tumor. J Clin Oncol 2008;26:4100–8.
17. Minakuchi Y, Takeshita F, Kosaka N, et al. Atelocollagen-mediated synthetic small interfering RNA delivery for effective gene silencing *in vitro* and *in vivo*. Nucleic Acids Res 2004;32:e109.
18. Takeshita F, Minakuchi Y, Nagahara S, et al. Efficient delivery of small interfering RNA to bone-metastatic tumors by using atelocollagen *in vivo*. Proc Natl Acad Sci U S A 2005;102:12177–82.
19. Shi L, Reid LH, Jones WD, et al. The MicroArray Quality Control (MAQC) project shows inter- and intraplatform reproducibility of gene expression measurements. Nat Biotechnol 2006;24:1151–61.
20. Bolker BM, Brooks ME, Clark CJ, et al. Generalized linear mixed models: a practical guide for ecology and evolution. Trends Ecol Evol 2009;24:127–35.
21. Gardina PJ, Clark TA, Shimada B, et al. Alternative splicing and differential gene expression in colon cancer detected by a whole genome exon array. BMC Genomics 2006;7:325.
22. Hussain SP, Schwank J, Staib F, Wang XW, Harris CC. TP53 mutations and hepatocellular carcinoma: insights into the etiology and pathogenesis of liver cancer. Oncogene 2007;26:2166–76.
23. Gouas D, Shi H, Hainaut P. The aflatoxin-induced TP53 mutation at codon 249 (R249S): biomarker of exposure, early detection and target for therapy. Cancer Lett 2009;286:29–37.
24. Villanueva A, Newell P, Chiang DY, Friedman SL, Llovet JM. Genomics and signaling pathways in hepatocellular carcinoma. Semin Liver Dis 2007;27:55–76.
25. Katoh H, Shibata T, Kokubu A, et al. Genetic inactivation of the APC gene contributes to the malignant progression of sporadic hepatocellular carcinoma: a case report. Genes Chromosomes Cancer 2006;45:1050–7.
26. Shao J, Zhou B, Chu B, Yen Y. Ribonucleotide reductase inhibitors and future drug design. Curr Cancer Drug Targets 2006;6:409–31.
27. Gruss OJ, Vernos I. The mechanism of spindle assembly: functions of Ran and its target TPX2. J Cell Biol 2004;166:949–55.
28. Bayliss R, Sardon T, Ebert J, Lindner D, Vernos I, Conti E. Determinants for Aurora-A activation and Aurora-B discrimination by TPX2. Cell Cycle 2004;3:404–7.
29. Marumoto T, Zhang D, Saya H. Aurora-A—a guardian of poles. Nat Rev Cancer 2005;5:42–50.
30. Keen N, Taylor S. Aurora-kinase inhibitors as anticancer agents. Nat Rev Cancer 2004;4:927–36.
31. Harrington EA, Bebbington D, Moore J, et al. VX-680, a potent and selective small-molecule inhibitor of the Aurora kinases, suppresses tumor growth *in vivo*. Nat Med 2004;10:262–7.
32. Anderson K, Yang J, Koretke K, et al. Binding of TPX2 to Aurora A alters substrate and inhibitor interactions. Biochemistry 2007;46:10287–95.
33. Gerlich D, Hirota T, Koch B, Peters JM, Ellenberg J. Condensin I stabilizes chromosomes mechanically through a dynamic interaction in live cells. Curr Biol 2006;16:333–44.
34. Lam WW, Peterson EA, Yeung M, Lavoie BD. Condensin is required for chromosome arm cohesion during mitosis. Genes Dev 2006;20:2973–84.
35. Scuric Z, Stain SC, Anderson WF, Hwang JJ. New member of aldose reductase family proteins overexpressed in human hepatocellular carcinoma. Hepatology 1998;27:943–50.
36. Teramoto R, Minagawa H, Honda M, et al. Protein expression profile characteristic to hepatocellular carcinoma revealed by 2D-DIGE with supervised learning. Biochim Biophys Acta 2008;1784:764–72.
37. Li CP, Goto A, Watanabe A, et al. AKR1B10 in usual interstitial pneumonia: expression in squamous metaplasia in association with smoking and lung cancer. Pathol Res Pract 2008;204:295–304.

GASTROENTEROLOGY 2011;140:596–607

Prostaglandin E_2 Signaling and Bacterial Infection Recruit Tumor-Promoting Macrophages to Mouse Gastric Tumors

HIROKO OSHIMA,* KYOJI HIOKI,‡ BORYANA K. POPIVANOVA,* KEISUKE OGUMA,* NICO VAN ROOIJEN,§ TOMO-O ISHIKAWA,* and MASANOBU OSHIMA*

*Division of Genetics, Cancer Research Institute, Kanazawa University, Kanazawa; ‡Gnotobiology Laboratory, Central Institute for Experimental Animals, CIEA, Kawasaki, Japan; and §Department of Molecular Cell Biology, Vrije Universiteit, Amsterdam, The Netherlands

BACKGROUND & AIMS: *Helicobacter pylori* infection induces an inflammatory response, which can contribute to gastric tumorigenesis. Induction of cyclooxygenase-2 (COX-2) results in production of prostaglandin E_2 (PGE_2), which mediates inflammation. We investigated the roles of bacterial infection and PGE_2 signaling in gastric tumorigenesis in mice. **METHODS:** We generated a germfree (GF) colony of *K19-Wnt1/C2mE* mice (*Gan* mice); these mice develop gastric cancer. We examined tumor phenotypes, expression of cytokines and chemokines, and recruitment of macrophages. We also investigated PGE_2 signaling through the PGE_2 receptor subtype 4 (EP4) in *Gan* mice given specific inhibitors. **RESULTS:** *Gan* mice raised in a specific pathogen-free facility developed large gastric tumors, whereas gastric tumorigenesis was significantly suppressed in GF-*Gan* mice; reconstitution of commensal flora or infection with *Helicobacter felis* induced gastric tumor development in these mice. Macrophage infiltration was significantly suppressed in the stomachs of GF-*Gan* mice. *Gan* mice given an EP4 inhibitor had decreased expression of cytokines and chemokines. PGE_2 signaling and bacterial infection or stimulation with lipopolysaccharide induced expression of the chemokine C-C motif ligand 2 (CCL2) (which attracts macrophage) in tumor stromal cells or cultured macrophages, respectively. CCL2 inhibition suppressed macrophage infiltration in tumors, and depletion of macrophages from the tumors of *Gan* mice led to signs of tumor regression. Wnt signaling was suppressed in the tumors of GF-*Gan* and *Gan* mice given injections of tumor necrosis factor-α neutralizing antibody. **CONCLUSIONS: Bacterial infection and PGE_2 signaling are required for gastric tumorigenesis in mice; they cooperate to up-regulate CCL2, which recruits macrophage to gastric tumors. Macrophage-derived tumor necrosis factor-α promotes Wnt signaling in epithelial cells, which contributes to gastric tumorigenesis.**

Keywords: Stomach Cancer; Tumor Promotion; Bacterial Infection.

Gastric cancer is the second most common cause of cancer-related death in the world, and *Helicobacter pylori* infection is closely associated with gastric cancer development.[1] Infections are estimated to be related to 15% of malignant cancer development, and infection-associated inflammation is a critical component of cancer development.[2] For example, an inflammatory response promotes tumor cell proliferation, metastasis, and survival, whereas it suppresses antitumor immune responses.[2–4] Moreover, the genetic polymorphisms in genes encoding inflammatory cytokines influence gastric tumorigenesis.[5] These results suggest that an inflammatory cytokine network induced by *H pylori* infection plays a key role in gastric tumorigenesis.

Cycooxygenase-2 (COX-2) is an inducible enzyme for prostaglandin biosynthesis, which plays an important role in both inflammation and tumorigenesis.[6,7] Mouse model studies have indicated that induction of the COX-2/prostaglandin E_2 (PGE_2) pathway accelerates intestinal tumorigenesis through the induction of angiogenesis and suppression of apoptosis.[8,9] Among 4 PGE_2 receptors (EP1–EP4), EP4 receptor signaling has been shown to play an important role in intestinal tumorigenesis through the activation of epidermal growth factor receptor.[10] The expression of COX-2 is also found in more than 70% of gastric cancers,[11] which is suppressed by the eradication of *H pylori*,[12] suggesting COX-2 induction by infection in the gastric mucosa. Transgenic mice expressing COX-2 and a PGE_2 converting enzyme, microsomal prostaglandin E synthase-1 (mPGES-1), in the stomach develop hyperplasia with macrophage infiltration, indicating the role of PGE_2 in macrophage recruitment.[13] Tumor-associated macrophages (TAMs) play an important role in tumorigenesis through the enhancement of angiogenesis, migration, and remodeling.[14] Moreover, the simultaneous activation of Wnt and the PGE_2 pathways in the mouse stomach causes dysplastic tumor de-

Abbreviations used in this paper: COX-2, cyclooxygenase-2; *Gan*, Gastric neoplasia; GF, germfree; IL-1β, interleukin-1β; IL-6, interleukin-6; LPS, lipopolysaccharide; mPGES-1, microsomal prostaglandin E synthase-1; NF-κB, nuclear factor-κB; PGE_2, prostaglandin E_2; RT-PCR, reverse transcription-polymerase chain reaction; SPF, specific pathogen free; TAM, tumor-associated macrophage; TNF-α, tumor necrosis factor-α.

0016-5085/$36.00
doi:10.1053/j.gastro.2010.11.007

velopment.[15] Accordingly, it is possible that PGE_2-dependent macrophage recruitment is one of the important mechanisms underlying the *H pylori* infection-associated inflammation in gastric tumorigenesis. However, the relationship between bacterial infection and PGE_2 signaling in gastric tumorigenesis remains unclear.

Commensal bacteria constitutively stimulate the intestinal mucosa, inducing cytokines and chemokines at a basal level, which is important for homeostasis of the intestinal mucosa.[16] The present study shows that indigenous bacteria constitutively stimulate the gastric mucosa, which is required for tumorigenesis in the Wnt-activated and PGE_2-induced gastric mucosa. Bacterial colonization and PGE_2 signaling through EP4 receptor cooperatively induced the expression of CCL2, which was a major pathway for macrophage recruitment in the gastric mucosa. Furthermore, depletion of macrophages caused regressive signs of tumors. These results indicate that bacterial infection and PGE_2 signaling cooperatively recruit macrophages to the gastric mucosa, which promotes gastric cancer development.

Materials and Methods

Animal Experiments

The construction of *K19-Wnt1* [*Tg(Krt19-Wnt1)2Maos*], *K19-C2mE* [*Tg(Krt19-Ptgs2,Krt19-Ptges)8Tko*], and *K19-Wnt1/C2mE* (*Gan* for Gastric neoplasia) [*Tg(Krt19-Wnt1)2Maos/Tg(Krt19-Ptgs2,Krt19-Ptges)8Tko*] transgenic mice was described previously (Supplementary Table 1).[13,15] All mice used in the present study were backcrossed to C57BL/6 mice more than 12 times. Germfree (GF) mouse colonies of all genotypes and wild-type mice were established by cesarean derivation at the Central Institute for Experimental Animals (CIEA, Kawasaki, Japan), and the mice were raised in GF isolators under GF conditions. During the experiments, GF conditions were monitored by cultures of feces, bedding, and swabs in thioglycollate medium or potato dextrose broth every 2–5 weeks (Supplementary Table 2). Specific pathogen free (SPF)-raised mice were maintained in the SPF facility at Kanazawa University. The excluded pathogens in the SPF facility are listed in Supplementary Table 3. Mice were killed and examined at 30 and 55 weeks of age (n = 4–6 mice), and all experimental groups consisted of both female and male mice. Half of the glandular stomach was used for the histologic analysis, and the other half was used for RNA and protein sample preparation. Six GF *Gan* mice were moved to the SPF facility at 7 weeks of age, reconstituted with commensal flora by cohousing with SPF mice and adding dirty bedding from other cages and examined at 30 weeks of age. *Helicobacter felis* (ATCC 49179) were inoculated at 10^8/mouse PO to GF *Gan* mice at 30 weeks of age (n = 3 mice), and gastric phenotypes were examined at 55 weeks of age. The time course and experimental conditions for each group are shown in Supplementary Figure 1. All animal experiments were carried out according to the protocol approved by the Committee on Animal Experimentation of Kanazawa University.

Gastric pH Measurement

Gastric pH was measured as described.[17] Briefly, mice were fasted overnight before necropsy. Sterile water (1.5 mL) was injected into the stomach, the stomach was massaged gently, and the pH of the gastric contents was measured using a pH meter.

Drug Treatment Experiments

The EP4 receptor inhibitor RQ-00015986/CJ-42794[18] was provided from RaQualia Pharma Inc (Taketoyo, Japan). *Gan* mice were treated with RQ-00015986 at 100 mg/kg/day PO from 27 or 52 weeks of age for 3 weeks (n = 4 or 5 mice). For inhibition of tumor necrosis factor (TNF)-α or CCL2, *Gan* mice were injected with a neutralizing antibody against TNF-α (AB-410-NA; R&D Systems, Minneapolis, MN) at 8 mg/kg/day intraperitoneally for 6 days (n = 3 mice) or an antibody against CCL2 (AF-479-NA; R&D Systems) at 1 mg/kg/day intraperitoneally for 3 days (n = 3 mice), respectively. Macrophages were depleted in vivo by injection of 200 μL clodronate (dichloromethylene bisphosphonate)-loaded liposomes intravenously every 3 days for 2 weeks as previously described.[19] Clodronate was a gift from Roche Diagnostics GmbH (Mannheim, Germany) and was encapsulated in liposomes as described previously.[20]

Histology and Immunohistochemistry

Stomach tissues were fixed in 4% paraformaldehyde, paraffin embedded, and sectioned at 4-μm thickness. These sections were stained with H&E or processed for immunostaining. Tissues were also embedded in OCT compound (Sakura Finetechnical, Tokyo, Japan), frozen in liquid nitrogen, and sectioned at 10-μm thickness. The frozen sections were used for CCL2 immunostaining. Antibodies against the proton pump (MBL, Nagoya, Japan), F4/80 (Serotec, Oxford, UK), β-catenin (Sigma, St. Louis, MO), CCL2 (Hycult Biotech, Uden, The Netherlands), EP4 (MBL), CD44 (Millipore, Billerica, MA), EphB3 (Bioworld Technology, St. Louis Park, MN), and Ki-67 (Dako, Carpinteria, CA) were used as the primary antibodies. Staining signals were visualized using the Vectastain Elite Kit (Vector Laboratories, Burlingame, CA). For fluorescence immunostaining, Alexa Fluor 594 or Alexa Fluor 488 antibody (Molecular Probes, Eugene, OR) was used as the secondary antibody. Apoptosis was examined using the ApopTag Apoptosis Detection Kit (Millipore). The mean index for F4/80 (macrophage), proton pump (parietal cell), Ki-67, or apoptosis was calculated by counting labeled cells per microscopic field (200×) in 5 fields.

Scoring Tumor Volume and Preneoplastic Lesions

The mucosal thickness (tumor height) of the gastric tumors of *Gan* mice and the normal stomach of wild-type mice was measured from histology sections. The mucosal thickness relative to that of wild-type mice was calculated. The number of preneoplastic lesions in the whole glandular stomach of *K19-Wnt1* mice was counted under a dissection microscope after staining with 0.05% toluidine blue. The histologic characteristics of gastric tumors and preneoplastic lesions were described previously.[15] The histology of these lesions was confirmed after scoring.

Cell Culture Experiments

The RAW264 macrophage cells (RIKEN BioResource Center, Tsukuba, Japan) were treated with lipopolysaccharide (LPS) (Sigma) for 24 hours at 1, 10, 50, 100, 1000, or 10,000 pg/mL with or without treatment with a COX-2 inhibitor, celecoxib, or RQ00015986 at 10 μmol/L, and the expression levels of CCL2 and cytokines were examined. Celecoxib was provided by Pfizer (New York, NY). For the primary culture of gastric epithelial cells, the glandular stomach of *K19-Wnt1* mice was treated with 0.1% collagenase followed by trypsin, and epithelial cells were cultured in matrigel (BD Pharmingen, Franklin Lakes, NJ) with epidermal growth factor (EGF) (−) primary culture medium.[13] The primary cultured cells were treated with RQ00015986 at 10 μmol/L for 6 days, and organoid structures consisting of epithelial cells larger than 0.2 mm in diameter were counted.

Immunoblotting Analysis

The tissues were homogenized and sonicated in lysis buffer. Thereafter, the specimens were centrifuged at 20,000*g*, and 10 μg of the supernatant protein sample was separated in a 10% sodium dodecyl sulfate-polyacrylamide gel. An antibody against unphosphorylated active β-catenin (Millipore) was used as the primary antibody. Anti-β-actin (Sigma) was used as the internal control. The ECL detection system (GE Healthcare, Buckinghamshire, UK) was used to detect the signals.

Real-Time Reverse-Transcription Polymerase Chain Reaction

Tumor stroma and epithelial cell samples were separately collected from frozen sections using Laser Microdissection (Leica, Wetzlar, Germany). Total RNA was extracted from the tissues or microdissected samples using ISOGEN (Nippon Gene, Tokyo, Japan), reverse transcribed with PrimeScript RT reagent Kit (Takara, Tokyo, Japan), and polymerase chain reaction (PCR) amplified by Stratagene Mx300P (Agilent Technologies, Santa Clara, CA) using SYBR Premix ExTaqII (Takara). Primers for the real-time reverse-transcription polymerase chain reaction (RT-PCR) were purchased (Takara), and the primer sequences are shown in Supplementary Table 4.

Statistical Analysis

The data were analyzed using the unpaired *t* test and are presented as the means ± standard deviation. A value of $P < .05$ was considered to be statistically significant.

Results

Constitutive Stimulation of Gastric Mucosa by Indigenous Bacteria

To determine whether indigenous bacteria in the stomach stimulate the gastric mucosa, we examined the expression of cytokines and chemokines in the glandular stomach of germfree (GF) wild-type mice and control SPF mice by real-time RT-PCR (Figure 1*A*). Importantly, the expression levels of TNF-α, interleukin (IL)-1β, keratinocyte-derived chemokine (KC), and macrophage inflammatory protein-2 (MIP-2) decreased significantly in the GF mouse stomach compared with the SPF mice, whereas IL-6 expression slightly increased. These results indicate that commensal bacteria constitutively stimulate the gastric mucosa to induce inflammatory cytokines and chemokines at a basal level.

Gan mice were previously constructed by crossing *K19-Wnt1* and *K19-C2mE* mice (Supplementary Table 1).[13,15] We examined the number of parietal cells by immunostaining and measured intragastric pH in these models because bacterial growth is affected by intragastric acidity. The mean parietal cell index was similar in all strains, and the intragastric pH was around 3.5 (Figure 1*B–D*). However, in the dysplastic tumors of *Gan* mice, the number of parietal cells decreased significantly, and intragastric pH increased at 50–55 weeks of age. These results indicate that gastric acidity is not changed in *Gan* mice at early stages of disease compared with other models until large tumors develop at the later stages.

Suppression of Gastric Tumorigenesis in GF Mice

Gan mice raised in an SPF facility (SPF-*Gan*) developed large gastric tumors by 55 weeks of age (Figure 2*A* and *B*), and the mean tumor height increased to approximately 1.5-fold when compared with that at 30 weeks of age. In contrast, gastric tumorigenesis was significantly suppressed in the GF *Gan* (GF-*Gan*) mice, and the mean mucosal thickness of GF-*Gan* mice was less than 40% of the age-matched SPF-*Gan* mice (Figure 2*A* and *B*, Supplementary Figure 2). Approximately 40% of the SPF-*Gan* mice showed a moribund phenotype and thus were killed by 60 weeks of age, whereas all GF-*Gan* mice survived by 55 weeks of age (Figure 2*C*). Importantly, reconstitution of commensal bacteria in GF-*Gan* mice resulted in development of gastric tumors that were significantly larger than those of GF-*Gan* mice (Figure 2*A*, Supplementary Figure 2), and treatment of SPF-*Gan* mice with antibiotics significantly suppressed gastric tu-

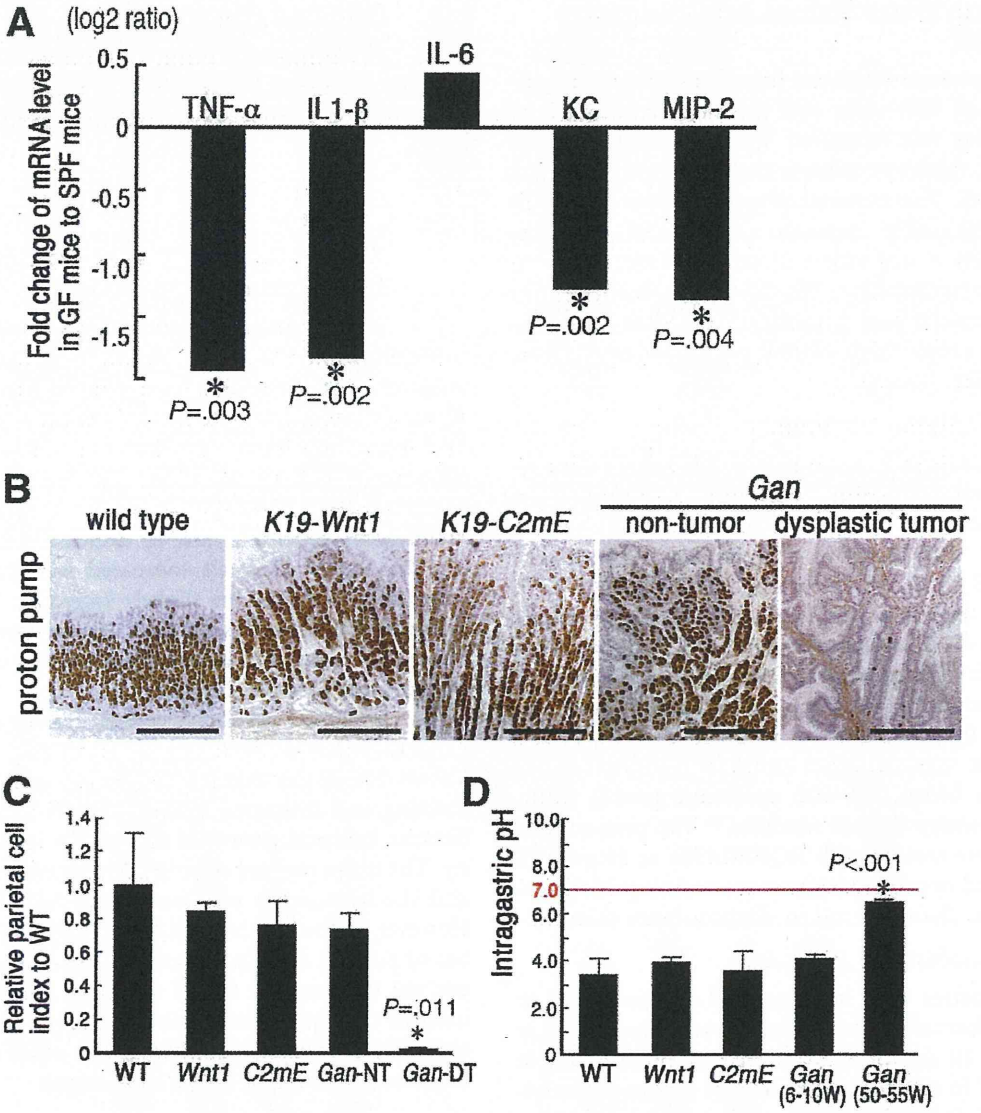

Figure 1. Stimulation of normal gastric mucosa by indigenous bacteria. (*A*) Messenger RNA (mRNA) levels of cytokines and chemokines in the gastric mucosa of the germfree (GF)-wild-type mice (mean log2 ratio to the SPF mouse level). *$P < .05$. (*B*) Immunostaining for proton pumps (parietal cells) in the gastric mucosa of the indicated strains. *Scale bars*, 100 μm. (*C*) The parietal cell index relative to the wild-type mouse level (mean ± standard deviation [SD]). *$P < .05$ vs the wild-type level (*WT*). *Gan*-NT, *Gan* nontumor; *Gan*-DT, *Gan* dysplastic tumor. (*D*) Intragastric pH of the indicated mouse strains (mean ± SD). *$P < .001$ vs the wild-type level (*WT*).

mor growth (Supplementary Figure 3). These results indicate that colonization of indigenous bacteria is required for gastric tumor development.

Moreover, infection with *Helicobacter felis*, separate species of *Helicobacter pylori*, in the GF-*Gan* mouse stomach at 30 weeks of age (GF->*H felis* mice) induced the development of gastric tumors by 55 weeks of age (Figure 2*A* and *B*). The infection of *H felis* in gastric glands was confirmed by microscopy of histology sections (Supplementary Figure 4). These results also indicate the role of infection in gastric tumorigenesis.

Apoptotic cells were found only on the mucosal surface of gastric tumors (Figure 2*D*), and the mean apoptosis index was 42.4% and 40.0% on the mucosal surface in SPF-*Gan* and GF-*Gan* mice, respectively. On the other hand, the number of Ki-67-labeled proliferating cells was significantly lower in the GF-*Gan* mouse stomach (Figure 2*E* and *F*), suggesting that bacterial colonization contributes to the tumor cell proliferation.

Suppression of Gastric Tumorigenesis by Inhibition of the PGE$_2$ Receptor EP4

There are 4 PGE$_2$ receptors (EP1–EP4), and the expression level of EP4 was increased significantly in *Gan* mouse tumors.[21] SPF-*Gan* mice were thus treated with a specific EP4 inhibitor, RQ-00015986, for 3 weeks from 52

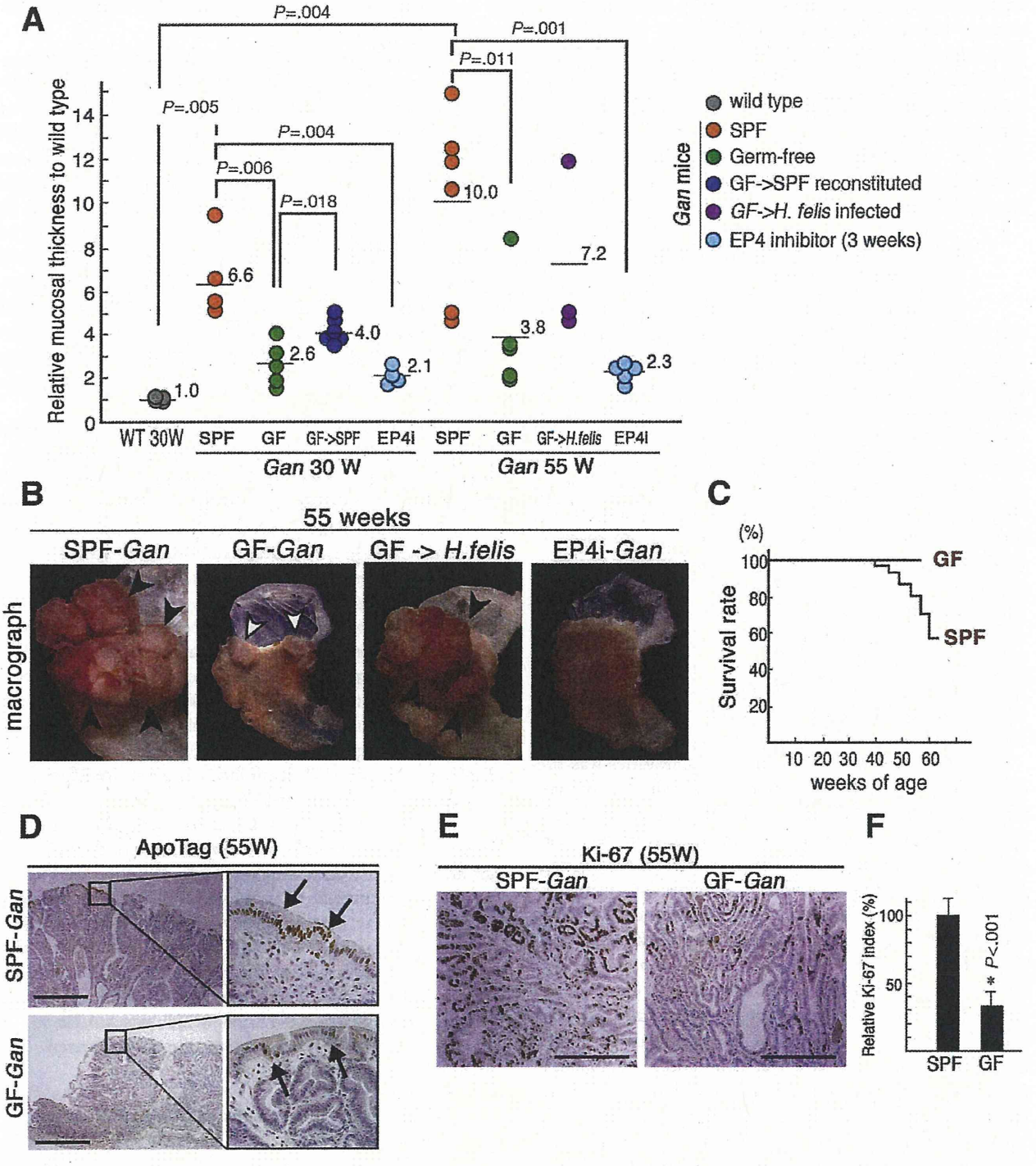

Figure 2. Suppression of gastric tumorigenesis in germfree (*GF*) *Gan* mice. (*A*) The gastric mucosal thickness (tumor height) of SPF-*Gan* (*SPF*), GF-*Gan* (*GF*), commensal flora-reconstituted GF-*Gan* (*GF->SPF*), *H felis*-infected GF-*Gan* (*GF->H felis*), and EP4 inhibitor-treated-*Gan* (*EP4i*) mice at 30 and 55 weeks of age relative to wild-type mice (*WT*). (*B*) Representative macroscopic photographs of the stomach of the indicated group of *Gan* mice at 55 weeks of age. *Black arrowheads* indicate tumors, whereas the *white arrowheads* indicate suppressed tumorous lesions in the *GF*-Gan mouse. (*C*) The survival rate of the SPF-*Gan* and GF-*Gan* mice. All GF-*Gan* mice were used for experiments at 55 weeks of age. (*D*) Apoptosis analyses of SPF-*Gan* and GF-*Gan* mouse gastric tumors. *Arrows* indicate apoptotic cells on the mucosal surface of tumors. (*E*) Ki-67 immunostaining in the gastric tumors of SPF-*Gan* and GF-*Gan* mice. *Scale bars* in *D* and *E*, 100 μm. (*F*) Relative mean Ki-67 labeling index (mean ± standard deviation). *$P < .001$ vs SPF level.

weeks of age (Supplementary Figure 1). Notably, gastric tumors regressed significantly following inhibition of EP4, and the mean tumor size decreased to 23% of that of the age-matched SPF-*Gan* mice (Figure 2*A* and *B*). Moreover, treatment of SPF-*Gan* mice with an EP4 inhibitor during the early stage of tumorigenesis from 27 weeks of age also suppressed tumor development significantly. These results indicate that EP4 signaling plays an important role in gastric tumorigenesis.

Bacterial Infection and EP4 Signaling for Inflammatory Responses

Submucosal lymphocyte infiltration was found in the SPF-*Gan* and GF->*H felis* mouse tumors but not in GF-*Gan* and EP4 inhibitor-treated *Gan* (EP4i-*Gan*) mice (Figure 3*A*), suggesting that both bacterial infection or colonization and EP4 signaling are required for inflammatory responses. Moreover, the expression level of proinflammatory cytokines, TNF-α, IL-1β, and IL-6 and chemokines, KC and MIP-2, were significantly elevated in the SPF-*Gan* and GF->*H felis* gastric tumors (Figure 3*B*), indicating inflammatory responses in the stomachs of these mice. In contrast, the expression of these cytokines and chemokines was not induced in the GF-*Gan* and EP4i-*Gan* mouse stomachs. The transgenic expression of COX-2 (*Ptgs2*) in the stomach was confirmed in all mouse groups except the wild-type mice, indicating that the PGE$_2$ level was elevated in all groups of *Gan* mice. These results indicate that both infection and EP4 signaling are required for inflammatory responses in the stomach.

The expression of proinflammatory cytokines was predominantly detected in stromal cells when compared with tumor epithelial cells in SPF-*Gan* tumors (Figure 3*C*), suggesting that stromal macrophages were the major source of these cytokines. We thus examined macrophage infiltration by immunostaining. As expected, numerous macrophages were found in the SPF-*Gan* and GF->*H felis Gan* mouse tumors, whereas macrophage infiltration was suppressed in the GF-*Gan* and EP4i-*Gan* mice (Figure 3*D*). The number of macrophages in the GF-*Gan* and EP4i-*Gan* mouse stomachs decreased significantly to 11% and 33% of the SPF-*Gan* mouse level, respectively (Figure 3*E*). These results suggest that cooperation of bacterial infection or colonization with EP4 signaling contributes to macrophage recruitment to the gastric mucosa.

To examine the role of macrophages in gastric tumorigenesis, SPF-*Gan* mice were treated with clodronate liposomes to deplete macrophages in vivo. Macrophage-depleted areas were found by immunostaining in the clodronate liposome-injected *Gan* mouse tumors (Figure 3*F*). In the macrophage-depleted area, tumors showed regressive signs with atrophic changes of tumor cells or peel-off of tumor epithelial cells from the mucosal surface, suggesting that macrophages are important for the maintenance or survival of tumor epithelial cells.

Induction of CCL2 by Bacterial Infection and EP4 Signaling

The expression level of macrophage-tropic chemokines was examined in the SPF-*K19-C2mE* and GF-*K19-C2mE* mouse stomach. The PGE$_2$ pathway but not Wnt signaling is activated in the glandular stomach of *K19-C2mE* mice (Supplementary Table 1). Importantly, expression of CCL2 and CCL8 increased significantly in the SPF-*K19-C2mE* mouse stomach compared with that in the wild-type mice (Figure 4*A*). In contrast, expression of CCL2 and CCL8 was not induced in the GF-*K19-C2mE* mouse stomach. Induction of CCL2 and CCL8 expression was also found in gastric tumors of SPF-*Gan* mice but not in GF-*Gan* mice (Figure 4*B*). These results suggest that PGE$_2$ signaling and bacterial colonization cooperatively induce expression of CCL2 and CCL8 in the gastric mucosa.

Because CCL2 is an important chemokine for macrophage infiltration in colon tumors,[22] we further examined CCL2 expression. CCL2-expressing cells were detected by immunostaining in the stroma of SPF-*Gan* mouse tumors where macrophages were accumulated (Figure 4*C*), suggesting that macrophages express CCL2. The stimulation of RAW264 macrophage cells with LPS induced the expression of CCL2 in a dose-dependent manner (Figure 4*D*). A low concentration of LPS was used for further experiments to examine the effect of low counts of indigenous bacterial colonization in the stomach. Importantly, treatment of RAW264 macrophages with an EP4 inhibitor significantly suppressed LPS-induced CCL2 expression (Figure 4*E*), suggesting that both EP4 signaling and LPS stimulation are required for CCL2 induction in macrophages.

To examine the role of CCL2 in macrophage recruitment in gastric tumors, SPF-*Gan* mice were treated with an anti-CCL2 neutralizing antibody. Notably, inhibition of CCL2 suppressed macrophage infiltration in tumors, although a few macrophages were still detected (Figure 4*F*), suggesting that CCL2 is a major chemokine that recruits macrophages to gastric tumors. In the macrophage-depleted tumor areas caused by CCL2 inhibition, tumors showed regressive signs, which was similar to the observations in the clodronate liposome-treated *Gan* mice (Figure 3*F*).

M2 Type Polarization of Macrophages in Gastric Tumors

TAMs play a pivotal role in tumor development.[14] Macrophage activation is classified as "classically" activated (M1) or "alternatively" activated (M2) type, and TAMs generally express characteristics of M2-polarized macrophages.[23] Interestingly, the expression of M2 macrophage markers, Ym1, Ym2, arginase 1 (Arg1), and transforming growth factor-β, increased significantly in both the SPF-*K19-C2mE* stomach and SPF-*Gan* tumors (Supplementary Figure 5*A*). Consistently, expression of